COMPUTATIONAL INTELLIGENCE AND MACHINE LEARNING
e-ISSN: 2582-7464

Computational Intelligence and Machine Learning
Vol-2, Issue-2, October 2021

Land use Land Cover Study of Sentinel-2A and Landsat-5 Images using NDVI and Supervised Classification Techniques

Dr.Aziz Makandar[1], Shilpa Kaman[2]

[1] Professor, Dept. of Computer Science, KSAWU, Vijayapura, Karnataka, India.
[2] Research Scholar, Dept. of Computer Science, KSAWU, Vijayapura, Karnataka, India.

Abstract

Land Use Land Cover (LULC) change monitoring plays very significant role in planning, policy making, management programs required for development activities at regional levels of any country. This study is an attempt to monitor LULC change of Vijayapura taluk, Karnataka, India for the period of 25 years from 1995 to 2021 using Remote Sensing (RS) and Geographic Information System (GIS). Satellite Images from Sentinel-2A MSI (Multispectral Imager), Landsat-5TM (Thematic Mapper) are used to generate LULC maps. Vegetation Change in the study area is computed using Normalized Difference Vegetation Index (NDVI) and results show that vegetation rate is increased from 0.6% in 1995 to 27.5% in 2021. Supervised Classification is carried out by using Maximum Likelihood Classification (MLC). 5 major classes considered for classification are namely: Waterbodies, Cropland/Vegetation, Fallow Land, Built-up Area and Barren Land. ArcGIS software tool is used for implementing the proposed study. Google Earth Pro used for accuracy assessment which is done by taking ground truth values for corresponding Classifications. Results show that the proposed system is able to achieve 88.16% of overall accuracy.

Keywords

High Resolution, Land Use Land Cover, Maximum Likelihood Classification, Multitemporal, Normalized Difference Vegetation Index, Remote Sensing, Satellite Images, Supervised Classification.

INTRODUCTION

While the terms land use and land cover are often used interchangeably, each word has a distinct meaning. The surface layer on the earth, such as trees, urban infrastructure, water, bare soil, and so on, is referred to as land cover. The function of the land, for example, recreation, wildlife habitat, or agriculture, is referred to as land use. When used in conjunction with the term "Land Use Land Cover," it refers to the categorization or classification of human activities and natural elements on the landscape over time using proven empirical and statistical methods of analysis of suitable source materials. [1]. Monitoring land use and land cover change is important for ensuring sustainable development over a period of time, particularly when it leads to inefficient urban development policies and uncontrolled, sometimes anarchic urbanization, which are often linked to environmental threats. [1][2]. Remote sensing techniques are commonly used to identify and track objects or events, as well as to generate detailed charts, records, and statistical data from Earth Observation images in order to provide geo-information to policy makers, experts, and the general public. For this reason, Land Cover Land Use (LCLU) maps are a valuable source of geo-information [3]. Satellite based data is being widely used as a basis for generating valuable information for LULC in various research works [4][5][6][7]. Various techniques of LULC study and change detection have been developed and implemented over the last few decades in India and across the world [8][9][10][11][12] [13] and [14]. In the present study Multitemporal Satellite Images of Landsat-5TM of 30m resolution and high resolution(10m) Sentinel-2A are used for generating LULC patterns of the study area i.e. Vijayapura taluk situated in Karnataka, India.

Vijayapura is characterized by low rain fall, high temperature and very low forest area. Natural vegetation found here is dry deciduous or thorn type of forest and agriculture is the main stay of people [15]. Due to the introduction of ambitious projects from Government of Karnataka like-

- From Water Resources Ministry to Rejuvenate and Replenish Tanks to fill Tanks and there by increase the ground water level [16].
- Working plan of Vijayapuara Forest Division from 2012-13 to 2021-22 [15].

There are noticeable changes in the LULC patterns of study area which makes it more interesting. There has been no attempt made previously to study the LULC in the specified region therefore, the paper aims to utilize geospatial techniques to detect the LULC changes in Vijayapura taluk from 1995 to 2021.

Organization of paper: Section I gives the Introduction, Section II briefs about Study Area and Datasets used, Section III and IV explain the Methodology applied to carry out NDVI Calculation and Supervised Classification, Section V discuss the Results, Section VI is the Conclusion.

STUDY AREA AND DATA SET

Study Area

The present study is carried out in Vijayapuara taluk from Karnataka State, India which was earlier called as Bijapur and renamed by Government of Karnataka on 1/11/2014. The latitude and longitude coordinates of Vijayapura are $16^0 15' 47.35''$ N, $75^0 50' 03.47''$ E with an area approximately 953.7km^2 as shown in Figure 1. Vijayapura is 556m above sea level. The average annual temperature here is 26.5 °C and rainfall is around 718 mm or 28.3 inch per year [17]. Agriculture is the main source of livelihood in the study area and most of the population lies surrounding Vijayapuara city.

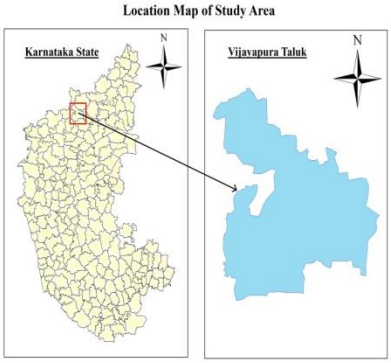

Figure -1: Location map of Vijayapura taluk, Karnataka, India.

Data Set

Multitemporal high resolution Sentinel-2A MSI imageries composed of 13 bands for the years 2015, 2021 and Landsat-5 TM imageries composed of 7 bands for the years 1995, 2008 are used for LULC mapping of study region. One of the main applications of Sentinel-2A and Landsat composite is for LULC analysis [18]. All Satellite Images used in the study are cloud free or with very less cloud coverage (within 10%) and are downloaded from open-source websites USGS earth explorer and Copernicus Open Access Hub. Vector data used in the study to get shape file for extracting Region of Interest is downloaded from Karnataka Geographic Information System (KGIS) website. Following table 1 gives the details of Satellite Images used.

SUPERVISED CLASSIFICATION

The aim of image classification is to extract features from remote sensing data by converting it into more concrete categories that reflect surface classes and conditions [19]. For remotely sensed image processing, classification is a commonly used research technique. There are three types of approaches in this collection: supervised, unsupervised, and hybrid.

Table-1: Details of Satellite Images used in the work.

Sl. No.	Satellite	Resolution and Bands used	Acquisition Dates	Source
1	Sentinel-2A MSI L2A	10m Bands B2, B3, B4, B8	26/01/2021	https://scihub.copernicus.eu/
2	Sentinel-2A MSI L1C	10m Bands B2, B3, B4, B8	24/12/2015	https://scihub.copernicus.eu/
3	Landsat- 5 TM L1TP	30m Bands B1 to B7	31/10/2008 - 145/48 09/12/2008 - 146/48	https://earthexplorer.usgs.gov/
4	Landsat- 5 TM L2SP	30m Bands B1 to B7	13/01/1995 - 145/48 20/01/1995 - 146/48	https://earthexplorer.usgs.gov/

The supervised classification method requires training samples to define each class. The unsupervised classification approach does not require any additional data because classes are defined solely by spectral value differences. The supervised and unsupervised classification methods are combined in the hybrid classification process [20]. The K-means, parallelepiped, ISODATA, MLC, and minimum distance to means are examples of traditional classification algorithms. MLC is the most precise classification scheme among them [21], as it is known as a reliable and robust classifier with high precision and accuracy. As a result, MLC is the most commonly used pixel-based method for classifying remotely sensed data [22] [23] [24].

MLC is a method for calculating the limit for a given statistic from a specified class of distributions. Electrical engineering can be traced back to the origins of MLC [25]. For the training samples, a normal distribution is assumed. The probability density functions for each group are generated by the algorithm. All unclassified pixels are assigned membership based on the relative likelihood (probability) of that pixel occurring within each category's probability density function during the classification process [26].

The process of classification used in this study is depicted in the following figure 2

Image Mosaicking: As there is no availability of single Satellite Image covering the study area, we have used two Landsat-5TM images of path 145/48 & 146/48 and mosaic them to get Region of Interest (ROI). The method of combining photographs of the same scene into a broad

picture is known as image mosaicking. The union of two input images would be the product of the image mosaic process [27].

In the present work ArcGIS geoprocessing tool Mosaic To New Raster is applied on 2 Landsat-5TM images of 1995 and 2008 to get single raster image [28].

Band Composite: Satellite Images are captured in multiple wavelengths of reflected light. We can combine different bands of image into picture for better interpretation [29]. Band composite of bands B2, B3, B4 and B8 with 10m resolution of Sentinel-2A images of 2015, 2021 and similarly Composite of bands B1 to B7 with 30m resolution of Landsat-5TM images of 1995, 2008 is performed on the input data set.

Extract ROI: Add vector data to extract ROI from the whole image using shape file.

MLC: Five major classes are considered for preparing LULC maps in the study area namely: Water Bodies, Cropland/Vegetation, Fallow Land which is pre-cultivated area, Built-up Area and Barren Land. MLC is applied on the extracted data sets to classify images.

- Training samples are selected for each class. Number of samples selected range from 30 to 100 depending upon particular class and image. For example, 25 to 30 samples for Water Bodies and 90 to 100 samples for Cropland.
- Create signature file and save training samples.
- Perform Maximum Likelihood Classification of input images using signature file.
- Calculate the area covered by each class.

Before selecting training samples Google Earth images are investigated carefully.

Accuracy Assessment: Overall accuracy of classified image is done by considering ground truth values from Google Earth Pro and comparing them with the point file created with random values in each class of the classified image.

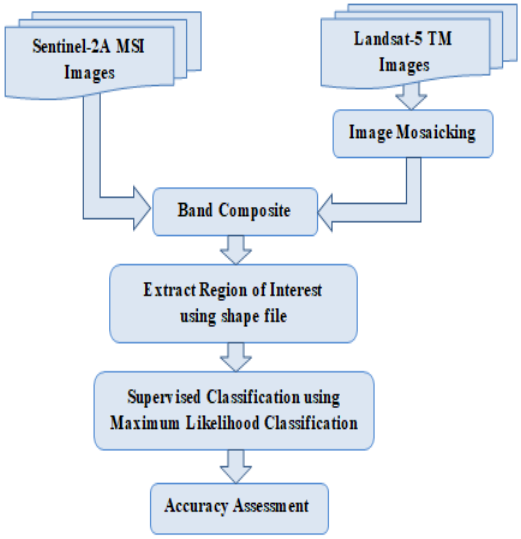

Figure -2: Flowchart of Classification process carried out in the study.

NDVI CALCULATION

The most widely used vegetation index is the normalized difference vegetation index (NDVI), which is a good indicator of large-scale vegetation cover and productivity [30]. The NDVI is a measure of vegetation health based on how plants reflect specific electromagnetic spectrum ranges. A plant appears green to the naked eye because its chlorophyll pigment reflects green waves when absorbing red waves. A stable plant with lots of chlorophyll and cell structures effectively absorbs red light and reflects near-infrared light. A sick plant can do the polar opposite [31]. It's used to improve the presence or absence of vegetation cover by generating the normalized band ratio [32]. The equation to calculate NDVI is defined as

$$NDVI = \frac{NIR - IR}{NIR + IR}$$

NIR stands for Near Infrared, and IR stands for Infrared. NDVI values range from +1 to -1, according to this equation. The non-vegetative surface is represented by negative values, while the green cover is represented by positive values, and the higher the positive values, the denser the green surface [32].

The process of NDVI calculation used in this study is shown in the figure 3.

- NDVI value for Sentinel-2A images is calculated with bands B4 & B8 using NDVI=(B8-B4)/(B8+B4).
- Similarly, for Landsat-5TM images NDVI is calculated with bands B3 & B4 using NDVI=(B4-B3)/(B4+B3).
- Images are classified into following 4 categories shown in table 2 based on values of NDVI.
- Combination of moderate and high values of vegetation are used to determine the vegetation change from 1995 to 2021.

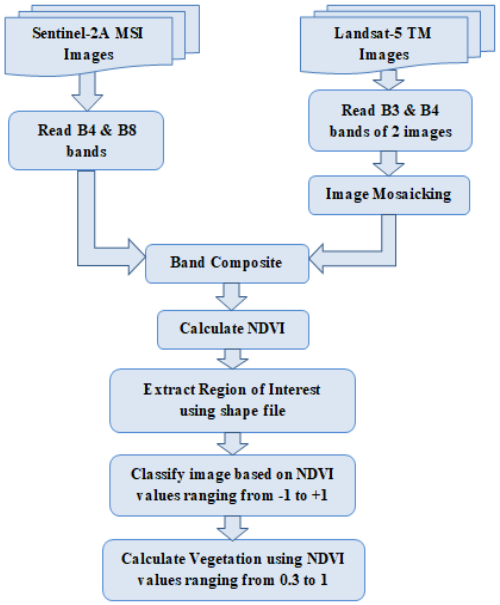

Figure -3: Flowchart for vegetation calculation using NDVI calculation.

Table -2: Vegetation classification with NDVI values.

Sl. No.	NDVI range	Vegetation
1	-1 to 0	Very low
2	0 to 0.3	Low
3	0.3 to 0.6	Moderate
4	0.6 to 1	High

RESULTS AND DISCUSSION

LULC Classification

Land Use Land Cover classification of Vijayapura taluk for multi temporal images of 1995, 2008, 2015 and 2021 covering five major classes namely: Water Bodies, Cropland/Vegetation, Fallow Land, Barren Land and Built-up Area are shown in figure 4. Results from classified maps indicate the spatial distribution of the area occupied by different classes from year 1995 to 2021 and corresponding changes in the LULC patterns which are highlighted with different colors in figure 4.

Values for LULC of different classes in terms of area covered in km^2 and changes in percentage is represented in table 3. Results show that area covered by Waterbodies is increased from 2.41 km^2 in 1995 to 6.82 km^2 in 2021 and Built-up Area is increased from 11.6 % in 1995 to 20.03% in 2021. Figure 5 shows the graph indicating visual changes for all 4 years from 1995 to 2021 in all 5 different classes more clearly.

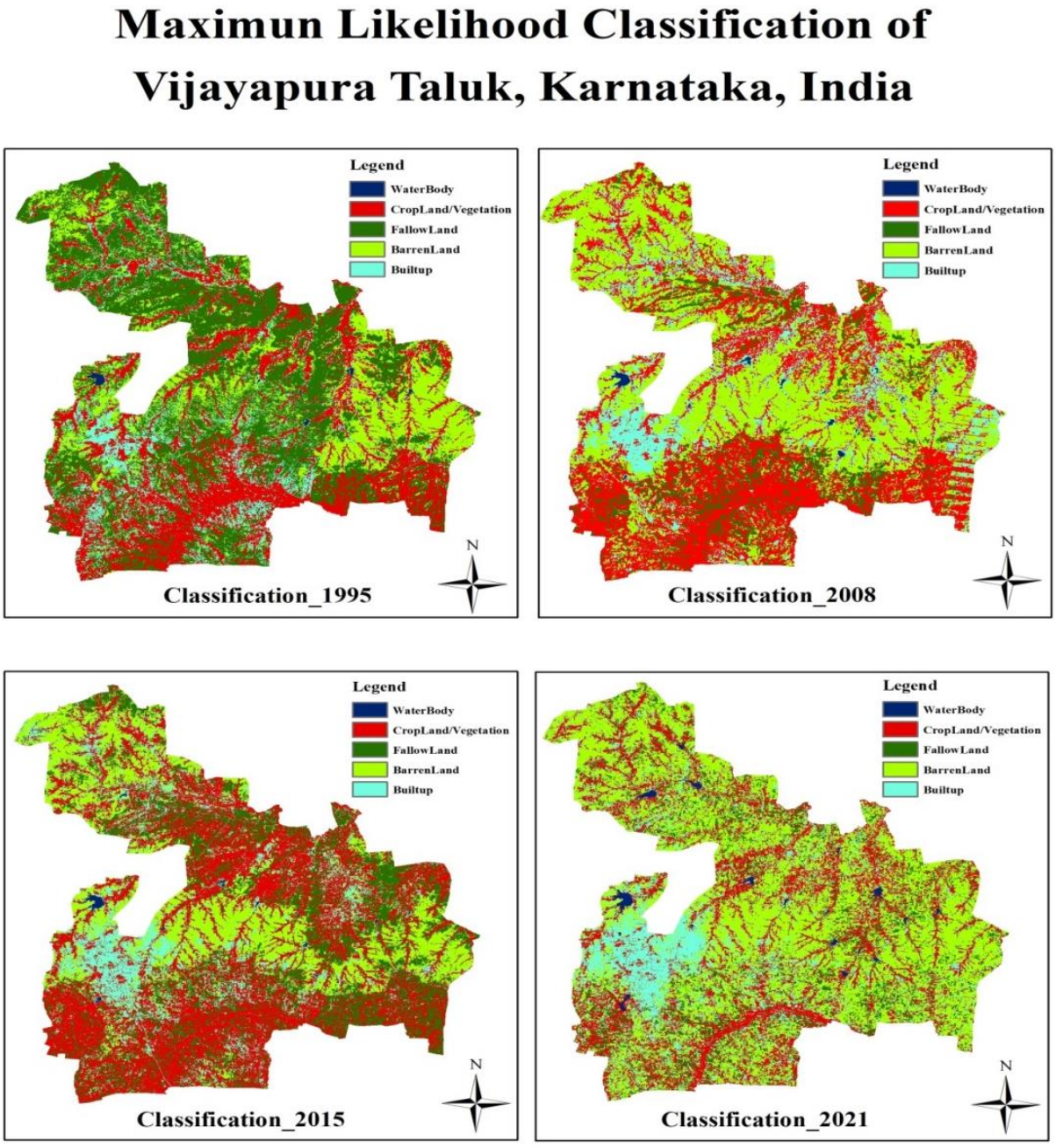

Figure -4: LULC change map for 1995, 2008, 2015 and 2021 of Vijayapura taluk, Karnataka, India.

Table -3: LULC distribution of Vijayapura taluk, Karnataka, India.

Sl. No.	LULC Classes	1995		2008		2015		2021	
		Area (km^2)	Area (%)	Area (km^2)	Area (%)	Area (km^2)	Area (%)	Area (km^2)	Area (%)
1	Water Bodies	2.41	0.25	3.45	0.36	2.84	0.29	6.82	0.71
2	Cropland/Vegetation	284.13	29.79	360.92	37.84	391.48	41.04	235.79	24.72
3	Fallow Land	386.42	40.51	100.05	10.49	219.14	22.97	114.63	12.01
4	Barren Land	170.15	17.84	349.74	36.67	194.38	20.38	405.4	42.5
5	Built-up Area	110.63	11.6	139.56	14.63	145.89	15.29	191.12	20.03
	Total	953.7	100	953.7	100	953.7	100	953.7	100

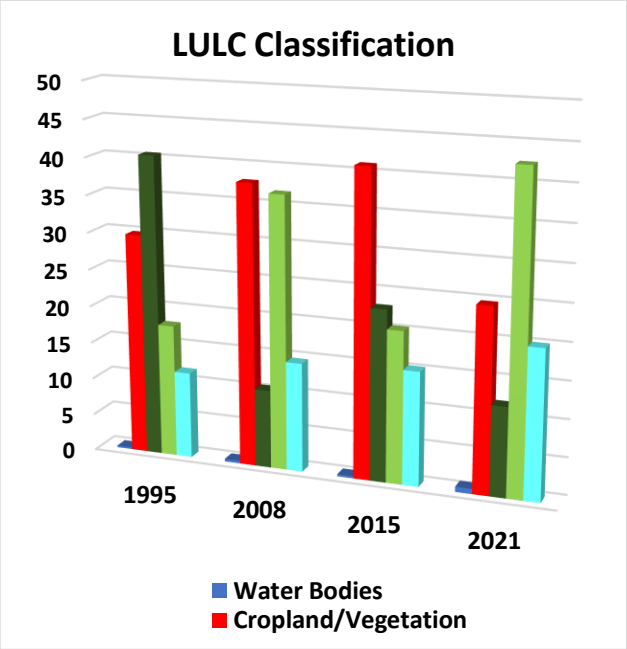

Figure -5: LULC changes during 1995, 2008, 2015 and 2021.

Accuracy Assessment

Accuracy Assessment is done by using error matrix by considering points in the classified image as user values and mapping those points to real time map of Google Earth Pro which are considered as ground truth values and gives producer values.

Google Earth is a strong and appealing source of positional data that can be used for research and preliminary studies with sufficient precision and at a low cost. Data availability that allows users from various disciplines to collaborate in order to extract positional data. Google Earth encourage experts to conduct research in order to test and evaluate positional data derived from Google Earth. [32].

Error matrix for overall accuracy of classified images from 1995 to 2021 is represented in the table 4 by considering 245 points which is equal to 88.16%. Table shows that water bodies, Built-up Areas are classified clearly and major misclassified points are from Cropland to Fallow land. Accuracy for individual year is calculated similarly using error matrix and the corresponding values are 85.71% in 1995, 91.8% in 2008, 85% in 2015, 90.16% in 2021 respectively.

Table -4: Error Matrix to Calculate Overall Accuracy of classification from 1995 to 2021.

LULC Class	Water Bodies	Crop Land/Vegetation	Fallow Land	Barren Land	Built-up Area	Total (User)
Waterbody	46	0	1	1	0	48
Crop Land	0	39	9	0	0	48
Fallow Land	0	6	41	1	0	48
Barren Land	0	1	3	47	0	51
Built-up Area	0	2	3	2	43	50
Total (Producer)	46	48	57	51	43	245

$$Overall\ Accuracy = \frac{Total\ number\ of\ correctly\ classified\ pixels}{Total\ number\ of\ referance\ pixels} \times 100$$

$$= \frac{216}{245} \times 100 = 88.16\%$$

Vegetation Calculation with NDVI

NDVI distribution of study area for the years 1995, 2008, 2015 and 2021 for Very low, Low, Moderate and High vegetation classes is shown in layout figure 7. Corresponding graph representing the comparison of NDVI change is shown

in figure 6. Results from classified maps show that there is increase in the vegetation from 0.69% in 1995, 12.15% in 2008, 17.13% in 2015 and 27.52% in 2021.Which means there is 26.83% growth in the vegetation during study period, this growth is shown with the graph in figure 5.

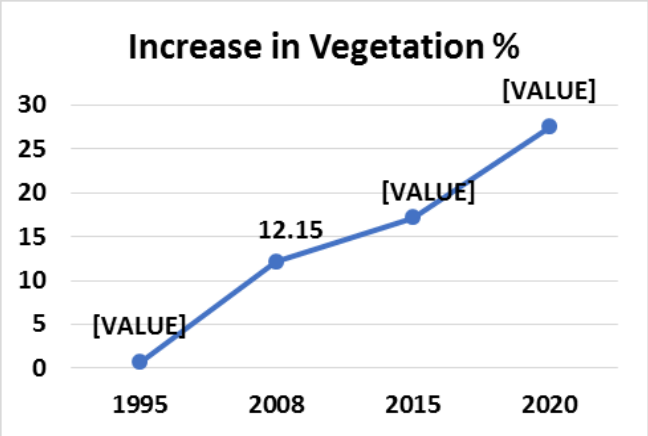

Figure -5: Increase in Vegetation from 1995 to 2021.

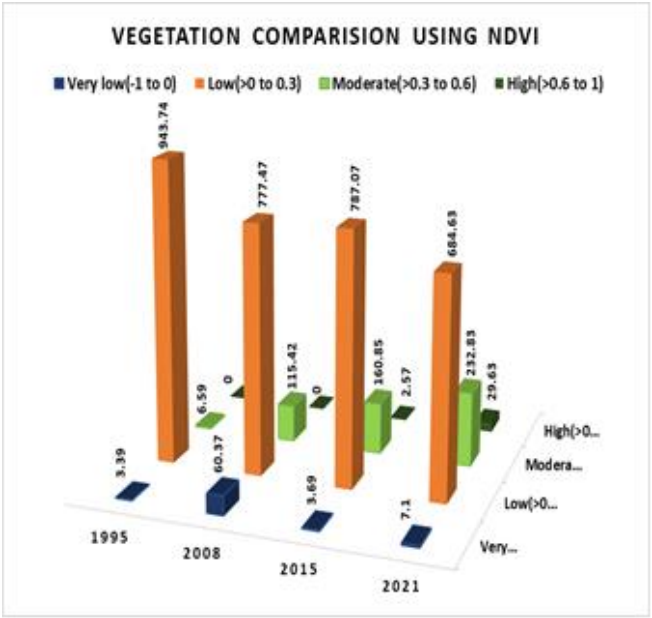

Figure -6: Compariosion of Vegetation Change from 1995 to 2021.

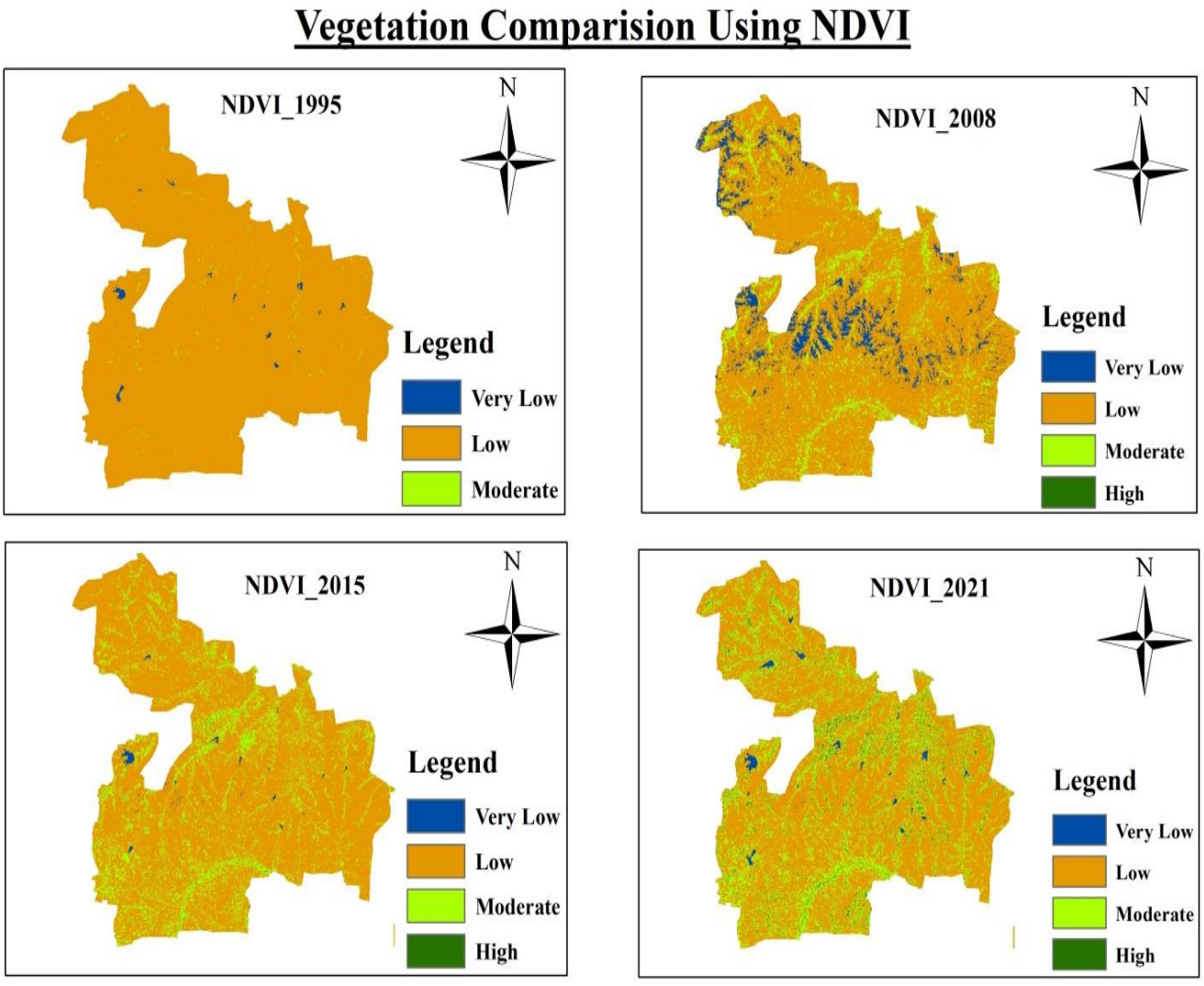

Figure -7: NDVI distribution layout for vegetation of Vijayapura taluk, Karnataka, India for 1995, 2008, 2015 and 2021.

CONCLUSION

The present study is the analysis of LULC change of Vijayapura taluk, Karnataka, India over the period from 1995 to 2021.Work is being carried out using multitemporal high resolution Sentinel-2A and Landsat-5TM images with the help of ArcGIS 10.5 software. Classification is done using pixel-based supervised classification scheme called MLC which is considered to be one of the most accurate, widely used algorithm. Results show that there is increase in Water Bodies from 2.41 km^2 to 6.82 km^2 due to Water Rejuvenate and Replenish plan, Built-up Area is increased from 11.6% to 20.03% due to urbanization, major area is covered by Cropland and Fallow land 70.3% in 1995, 48.33% in 2008, 64.01% in 2015 and 36.73% in 2021. Barren land is increased from 17.84% to 42.5% in 2021. Vegetation comparison is done using NDVI which shows there is increase in the vegetation from 0.69% in 1995 from 27.52% in 2021. Present study has achieved overall accuracy of 88.16% and as there are no previous works on LULC change done for Vijayapura taluk, results and interpretations of this work are critical for potential Land Use Land Cover practices in the study region.

The spatio-temporal analysis is being done by using RS and GIS techniques which is otherwise very tedious work using conventional mapping techniques. The work can be further extended by using unsupervised classification techniques and by using NDVI values and other vegetation indices for classification to achieve more accurate results.

REFERENCES

[1] https://www.satpalda.com/blogs/significance-of-land-use-land-cover-lulc-maps
[2] Barakat, A., Ouargaf, Z., Khellouk, R. et al. Land Use/Land Cover Change and Environmental Impact Assessment in Béni-Mellal District (Morocco) Using Remote Sensing and GIS. Earth Syst Environ 3, 113–125 (2019).
[3] E. O. Yilmaz, B. Varol, R. H. Topaloglu, and E. Sertel, “Object-based classification of Izmir Metropolitan City by using Sentinel-2 images,” in 2019 9th International Conference on Recent Advances in Space Technologies (RAST), pp. 407–412, Istanbul, Turkey, June 2019.
[4] Saadat, H., Adamowski, J., Bonnell, R., Sharifi, F., Namdar, M., Ale-Ebrahim, S., 2011. Land use and land cover classification over a large area in Iran based on single date analysis of satellite imagery. ISPRS J. Photogrammetry Remote Sens. 66, 608–619.
[5] Yuan,F., Sawaya, K.E., Loeffelholz, B., Bauer, M.E., 2005. Land cover classification and change analysis of the Twin Cities (Minnesota) Metropolitan Area by multitemporal Landsat remote sensing. Remote Sens. Environ. 98, 317–328.
[6] Hathout S., 2002. The use of GIS for monitoring and predicting urban growth in East and West St Paul, Winnipeg, Manitoba, Canada. J. Environ. Manage. 66, 229–238.
[7] Herold, M., Gardner, M.E., Robert, D.A., 2003. Spectral resolution requirements for mapping urban areas. IEEE Trans. Geosci. Remote Sens. 41, 1907–1919.
[8] Mishra P. K., Rai A, Rai S. C. Land use and land cover change detection using geospatial techniques in the Sikkim Himalaya, India, The Egyptian Journal of Remote Sensing and Space Science, Volume 23, Issue 2, 2020, Pages 133-143, ISSN 1110-9823.
[9] Wu,T., Luo, J., Fang, J., Ma, J., Song, X., 2018. Unsupervised object-based change detection via aWeibull mixturemodel-based binarization for high-resolution remote sensing images. IEEE Geosci. Remote Sens. Lett. 15, 63–67.
[10] Lv, Z., Liu, T., Wan, Y., Benediktsson, J.A., Zhang, X., 2018. Post-processing approach for refining raw land cover change detection of very high-resolution remote sensing images. Remote Sens. 10, 472.
[11] Sekertekin, A., Marangoz, A.M., Akcin, H., 2017. Pixelbased classification analysis of land use land cover using sentinel-2 and landsat-8 data. Int. Arch. Photogrammetry Remote Sens. Spatial Information Sci. XLII-4/W6, 91–93.
[12] Yu, H., Joshi, P.K., Das, K.K., Chauniyal, D.D., Melick, D.R., Yang, X., Xu, J., 2007. Land use/cover change and environmental vulnerability analysis in Birahi Ganga subwatershed of the Garhwal Himalaya, India. Tropical Ecol. 48 (2), 241.
[13] Salazar, A., Baldi, G., Hirota, M., Syktus, J., McAlpine, C., 2015. Land use and land cover change impacts on the regional climate of non-Amazonian South America: a review. Glob. Planet. Change 128, 103–119.
[14] Phiri, D., Morgenroth, J., 2017. Developments in landsat land cover classification methods: a review. Remote Sens., 9.
[15] https://aranya.gov.in/new/newdownloads/WP/vijaypura%20working%20plan.pdf
[16] https://www.thehindu.com/news/national/karnataka/After-50-years-Begum-Talab-brims-with-life/article15478911.ece
[17] https://en.climatedata.org/asia/india/karnataka/vijayapura-2796/
[18] Varade, Divyesh & Sure, Anudeep & Dikshit, Onkar. (2018). Potential of Landsat-8 and Sentinel-2A Composite for Land Use Land Cover Analysis. Geocarto International. 34. 1-32. 10.1080/10106049.2018.1497096.
[19] Aziz Makandar, Shilpa Kaman “Remote Sensing of Satellie Images Using Digital Image Processing Techniques A Survey”, International Conference on Artificial Intelligence and Soft Computing (ICAISC-2021), ISBN: 978-93-88929-53-0.
[20] K. Liu, W. Shi, H. Zhang, A fuzzy topology-based maximum likelihood classification, ISPRS Journal of Photogrammetry and Remote Sensing 66 (11) (201) 103–114.
[21] S. Shlien, A. Smith, A rapid method to generate spectral theme classification of Landsat imagery, Remote Sensing of Environment 4 (1976) 67–77.
[22] P.V. Bolstad, T.M. Lillesand, Rapid maximum likelihood classification, Photogrammetric Engineering and Remote Sensing 57 (1) (1991) 67–74.
[23] F. Maselli, C. Conese, L. Petkov, et al., Inclusion of prior probabilities derived from a nonparametric process into the maximum-likelihood classifier, Photogrammetric Engineering and Remote Sensing 58 (2) (1992) 201–207.
[24] Jiabo Sun, Jianyu Yang, Chao Zhang, Wenju Yun, Jieqing Qu, Automatic remotely sensed image classification in a grid environment based on the maximum likelihood method, Mathematical and Computer Modelling, Volume 58, Issues 3–4, 2013, Pages 573-581, ISSN 0895-7177.
[25] J.N. Nilsson, Learning Machines: Foundations of Trainable Pattern-Classifying Systems, in: McGraw-Hill Series in Systems Science, McGraw-Hill Book Company, New York, 1965.
[26] O. Hagner, H. Reese, A method for calibrated maximum

likelihood classification of forest types, Remote Sensing of Environment 110 (4) (2007) 438–444.
[27] D.K. Jain, G. Saxena, V.K. Singh, Image mosaicing using corner techniques, in: International Conference on Communication Systems and Network Technologies (CSNT), 2012, pp. 79–84.
[28] https://desktop.arcgis.com/en/arcmap/10.3/manage-data/raster-and-images/what-is-a-mosaic.htm
[29] https://sagatutorials.wordpress.com/band-composite-rgb-display/
[30] Sun, J., Qin, X. Precipitation and temperature regulate the seasonal changes of NDVI across the Tibetan Plateau. Environ Earth Sci 75, 291 (2016).
[31] https://up42.com/blog/tech/5-things-to-know-about-ndvi
[32] Zomrawi, Nagi & Mohammed, & Ghazi, Ahmed & Mustafa, Hussam. (2013). Positional Accuracy Testing of Google Earth. 4. 2045-7057.